Numerical Analysis of the MM-Wave Scattering from Randomly Rough Surfaces

Yarovoy, Alexander; Bouwmeester, Wietse; Rufas, Elizabeth; Fioranelli, Francesco

DOI
10.1109/RADAR58436.2024.10993714

Licence
Dutch Copyright Act (Article 25fa)

Publication date
2024

Document Version
Final published version

Published in
International Radar Conference

Citation (APA)
Yarovoy, A., Bouwmeester, W., Rufas, E., & Fioranelli, F. (2024). Numerical Analysis of the MM-Wave Scattering from Randomly Rough Surfaces. In *International Radar Conference: Sensing for a Safer World, RADAR 2024* (Proceedings of the IEEE Radar Conference). IEEE. https://doi.org/10.1109/RADAR58436.2024.10993714

Numerical Analysis of the MM-Wave Scattering from Randomly Rough Surfaces

Alexander Yarovoy
Microwave Sensing, Signals and Systems
Delft University of Technology
Delft, the Netherlands
A.Yarovoy@tudelft.nl

Wietse Bouwmeester
Microwave Sensing, Signals and Systems
Delft University of Technology
Delft, the Netherlands
W.Bouwmeester@tudelft.nl

Elizabeth Rufas
Microwave Sensing, Signals and Systems
Delft University of Technology
Delft, the Netherlands
Bet.Rufas@gmail.com

Francesco Fioranelli
Microwave Sensing, Signals and Systems
Delft University of Technology
Delft, the Netherlands
F.Fioranelli @tudelft.nl

***Abstract*—A numerical model is developed in the electromagnetic software suite FEKO to simulate scattering from surfaces with pre-defined statistical properties. The model considers surface roughness profile, incident angle and source polarization. Statistical analysis of the scattered field is performed using the Monte Carlo method using full-wave scattering results from a statistical ensemble of rough surface realizations. The performance of the numerical model has been verified in the limiting case of small height and small slope surfaces by comparison with the small perturbation theory. By means of the model proposed, new insight in scattering from statistical surfaces with an averaged surface slope above 0,5 as well as non-Gaussian surface statistics has been obtained.**

Keywords*— *Rough surface scattering, full-wave simulation, Monte-Carlo method

I. Introduction

Wide deployment of mm-wave radars in road vehicles has attracted attention to mm-wave scattering from statistically rough surfaces, especially at grazing angles. With typical values of root-mean squared (RMS) height of fresh asphalt around 2-3mm and correlation lengths of the same order [1], such surfaces cannot be considered smooth (small height and possessing small slope). Consequently, previously developed analytical models such as the Small Perturbation Method [2], Kirchhoff scattering [2], and Small Slope Approximations [3, 4] are not applicable to road surfaces illuminated with 77-81GHz radars. Furthermore, combination of moderate slopes of road surfaces with grazing angle illumination (typical for automotive radars) should result in multiple acts of scattering of the same electromagnetic wave on different but still correlated heterogeneities of the rough surface. According to general understanding of the scattering from rough surfaces such scattering process should result in increase of the backscattering and appearance of the cross-polarized component in the backscattered field. Both effects could not be described qualitatively by available theoretical models. Several experimental studies demonstrated a large variety of locally-measured RCS values [5-9], which is probably caused by large variety of road surface profiles. In such situation, a generic numerical model for road RCS would be a useful tool to predict surface clutter for different road conditions, types of asphalt, frequencies and polarizations of the incident waves.

In this paper, a novel numerical model to compute RCS of statistically random surfaces is proposed. The model is based on full-wave simulations of electromagnetic wave scattering on an arbitrary-profiled surface and is further development of the pioneering work [10] from computational electromagnetics point of view. To keep the model easily transferable to different users, a commercial solver FEKO is used. Statistical analysis of RCS is performed using the Monte Carlo method using a statistical ensemble of rough surfaces. The model developed is applied to scattering of electromagnetic waves from moderately rough perfectly electrically conducting surfaces with Gaussian correlation function and different probability density functions (PDF) and new – in comparison with predictions of (semi-)analytical models – physical results are demonstrated.

II. Numerical Model

A. Geometrical model

In a custom-made solver, it would be possible to consider an infinite rough surface *S* and limit the illuminated area of it by using tapered incident wave [11]. This option does not exist in FEKO [12], where the surface *S* has to be an enclosure of volume *V*. For simplicity, the volume V was selected to have parallelepiped shape with a rough surface on its top facet (Fig. 1).

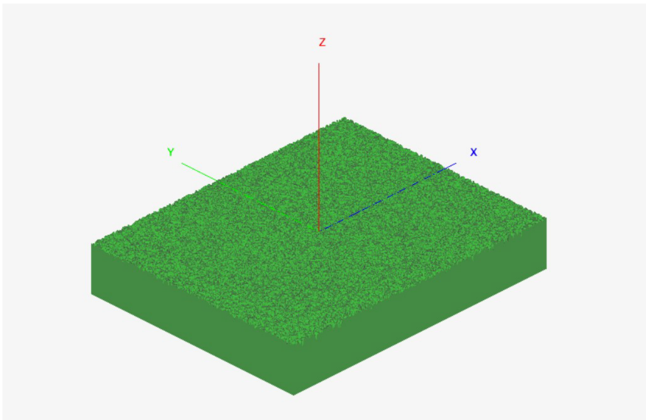

Fig. 1. The 3D view of the scattering volume with statistically rough upper surface.

The rough surface has been generated using a spectral filter and probability transforms to obtain a rough surface of prescribed size and with the same statistical distribution as targeted (Fig. 2). The procedure begins with the design of a spectral filter, which is based on the Gaussian autocorrelation function:

$$ACF = \exp\left(-\left(\frac{\sqrt{x^2+y^2}}{L}\right)^2\right)$$

Here *x* and *y* are the grid points in the X-Y plane, and *L* is the correlation length. This filter is then transformed to the spatial spectral domain by the Fourier transform (FT) to be used as a spectral filter. The second part of the procedure starts with

2024 International Radar Conference (RADAR) | 979-8-3503-6238-1/24/$31.00 ©2024 IEEE | DOI: 10.1109/RADAR58436.2024.10993714

creating a random white noise surface. The created surface is transformed into the spectral domain by the Fourier transform, so it can be filtered by the spectral filter to have the desired spectrum and autocorrelation function (Fig. 2). After adjusting the spectrum of the surface, the height distribution of the filtered surface needs to be adjusted to a targeted (in this particular case, exponential) distribution by probability transformation. The uniform distribution can be derived from the filtered surface using the following probability integral transformation:

$$P(Y \leq y) = P(F(x) \leq y) = P(x \leq F^{-1}(y))$$
$$= F(F^{-1}(y)) = y$$

Here Y=F(x) is the cumulative density function (CDF) of X, $F^{-1}(x)$ is the quantile function of X. Subsequently, the obtained uniform distribution Y is transformed to an exponential distribution by the inverse probability integral transformation, in this case by the logarithm Z= ln(Y/a)/b :

$$P(Z \leq z) = P(\frac{1}{b}\ln(\frac{Y}{a}) \leq y) = P(y \leq a\exp(by))$$

The adjusted surface follows the desired height distribution as well as correlation function. For further analysis, the RMS height can also be adjusted by applying scaling factors. Such procedure allows for the generation of an arbitrary surface with the specified surface dimensions, correlation length, and RMS height.

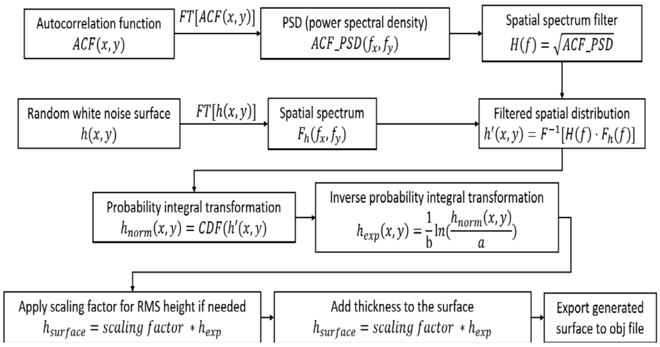

Fig. 2. Procedure of the random surface generation.

B. Electromagentic Field Source Configuration

To minimize the diffraction phenomena at the edges of the volume V, an amplitude-tapered incident wave has been used. To excite such a wave, a 2D binominal dipole array has been used (Fig. 3), in which the array factor AF is given by:

$$AF = 2a_1\cos(3kd\cos\varphi) + 2a_2\cos(2kd\cos\varphi)$$
$$+2a_3\cos(kd\cos\varphi) + a_4$$

Here d is the distance between neighbouring dipoles, which was selected to be equal to the half-wavelength, k is the wavenumber. The values of a_n can be defined as a binomial amplitude distribution between antenna elements resulting in a radiation pattern without sidelobes [13]. Using Maxwell-equation compatible incident wave with a footprint size equal to dozens of wavelength and dozens of correlation lengths reduces parasitic diffraction effects on the edges of the footprint and allows to compute statistically solid RCS values for rough surfaces with any statistics.

C. Numerical Solver

The scattering problem is formulated using the Surface Integral Method in frequency domain [10]. Compared with other numerical methods such as FDTD (Finite Difference Time Domain) and FEM (Finite Elements Method), the surface formulation requires less computational resources. For a perfectly electrically conducting surface, the scattering problem is formulated by means of Electrical Field Integral Equation which was solved by the Method of Moments using an MLFMM (Multilevel Fast Multipole Method). The MLFMM is used to solve scattering from electrically large bodies [10]. Furthermore, using trial-and-error approach, it was found that usage of the Sparse Approximate Inverse (SPAI) preconditioner prior to inversion of the impedance matrix helps to decrease the computational time while keeping the most accurate results.

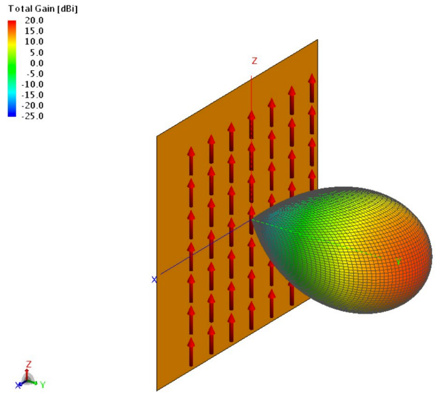

Fig. 3. The 3D view of the binominal dipole array radiation patterns.

D. Statistical Averaging

To separate the coherent and incoherent components of the scattered field scattered from a statistically rough surface and compute statistical moments of the latter, Monte Carlo simulations have been used over an ensemble of random realizations of this statistically rough surface. Due to the incident field footprint size of about 15 local heterogeneities of the surface (the footprint size increases with the incident angle), the convergence of the statistical moments of the scattered field was observed already by averaging over 7-12 realizations of rough surfaces. However, to get statistically accurate values, averaging over 25 random surface realizations has been used.

III. Numerical Results and Analysis

A. Adjusting the footprint size

Due to limited size of the scattering volume, it was important to adjust the incident field footprint size in such a way, that the amplitude of the field diffracted from the edges of the volume V will be several orders of magnitude smaller than the expected backscattered field. At the same time, the footprint size should be large enough to cover a number of surface heterogeneities sufficient for statistical averaging. These are assumed to have similar size than the correlation function of the rough surface. An example of the incident field footprint is given in Fig. 4 and the power reflected from the volume V with an ideally flat (even) upper surface is shown in Fig. 5. Based on numerical analysis it was found that the amplitude of the surface current excited at the edges of the volume V should be more than 40dB down in comparison with the one in the center of the footprint. This has resulted in selection of the values [1; 6; 15; 20] for the coefficients *a*, which determine the radiation patterns of the source, for the volume *V* with the size of 300mm*300mm*50mm by the incident angle of 45 degrees. For such source radiation patterns, the minimal footprint size was approximately equal to 15 correlation lengths of the rough surface. With increase of the incident angle to 60 degrees, due to increase of the footprint size, the volume *V* size has to be increased to 500mm*500mm*50mm, which increases essentially the computation time. In this paper, all numerical results are shown for the volume *V* size of 400mm*400mm*40mm with a moderately rough surface with the root mean square (RMS) height (unless opposite is stated) and correlation length both equal to 2mm. We considered an incident wave at a frequency of 77GHz, which impinges at the rough surface at the angle of -45 degrees, and simulated the bi-static scattered power averaged over the ensemble of surface realizations and normalized to the maximum of the power specularly reflected from an even surface (Fig. 5).

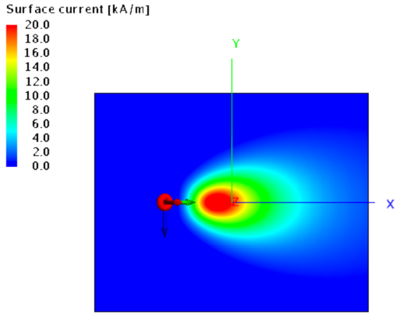

Fig. 4. The incident field footprint at the upper surface of the volume *V*.

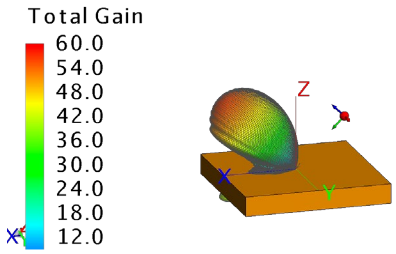

Fig. 5. The spatial distribution of the power of a horizontally polarized wave specularly reflected from an even surface.

B. Scattering from a Gaussian surface

As the majority of available numerical analysis for scattering from rough surfaces are available for surfaces with Gaussian PDF and autocorrelation function (Fig. 6), we started our analyses with scattering from a surface with Gaussian PDF.

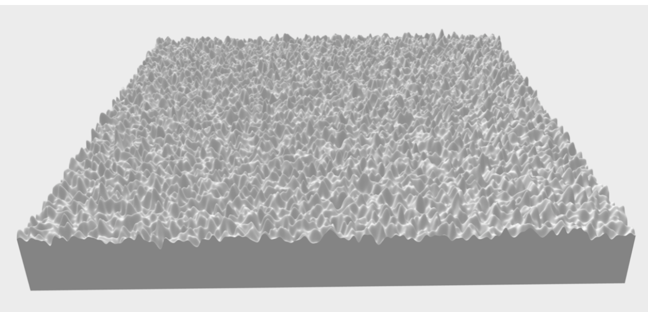

Fig. 6. Visualisation of the volume *V* with Gaussian upper surface.

We found that by 45 degrees incident angle the co- and cross-polarized scattered fields have similar values (Fig. 7), which have never been shown by all available (semi-)analytical models of scattering from rough surfaces. This can be interpreted as strong dominance of the multiple scattering process over single scattering processes as described by the majority of analytical models. Furthermore, the bi-static scattering patterns show almost isotropic scattering in all directions (similar to Lambert law).

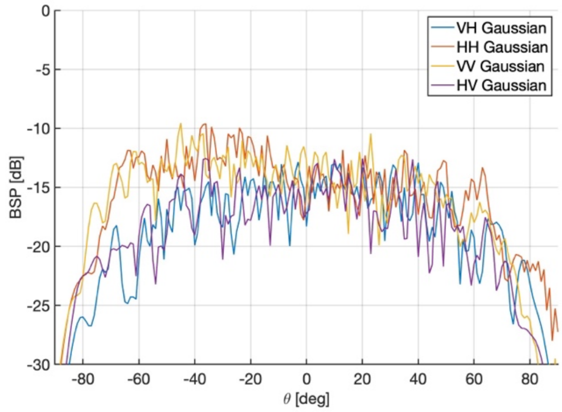

Fig. 7. Bi-static scattering from a rough surface with Gaussian PDF. The first index (H for horizontal, V for vertical) describes polarization of the scattered wave, while the second index describes incident wave polarization. The scattering angle θ is counted from the Z direction.

C. Exponential Surfaces

Particular attention was given to the numerical analysis of scattering from the surfaces with exponential PDF as such surface statistics together with Gaussian autocorrelation function has been experimentally determined for (fresh) asphalt surfaces [1]. In order to make a bridge to previously made analytical analysis, the field scattered from the smooth surfaces with RMS surface height of 0,2mm has been simulated firstly (Fig. 8). As expected, the power of the scattered field has a strong maximum in the direction of the forward scattering driven by the coherent component of the scattered field, which is reflected from the surface in specular direction. As it is also expected for the perfectly electrically conducting surface, there is no difference between the horizontally and vertically polarized incident field for the forward scattered field. For the backscattered field, the vertically polarized incident field produces slightly larger scattering, which is also in line with predictions of the small perturbation theory and small slope approximation. The cross-polarized component is considerably weaker than the co-polarized component in the plane of incidence (X-Z-plane), while the small perturbation theory predicts it to be exactly zero.

For moderately rough surfaces (in simulations, the surface RMS height equals 2mm with the surface correlation length of 2mm; in comparison with the results described above the statistical slope of the surface has been increased in 10 times), two effects are observed: (i) the bi-static scattering pattern shows almost isotropic scattering in all directions (Fig. 9), which is similar to Lambert law, (ii) the co- and cross-polarized backscattered fields have very similar values, which has never been shown by all available (semi-)analytical models of scattering from rough surface (Fig. 10). Both phenomena can be interpreted as strong dominance of the multiple scattering process over single scattering processes.

Both phenomena are essential for understanding the road clutter and its signature as observed by the automotive radars.

In comparison to the surface with Gaussian PDF (Fig. 7), almost 10dB increase of the total backscattered power for the surface with exponential PDF is observed (Fig. 10). This increase could be attributed to the larger density of surface slopes with higher values in case of the exponential statistics.

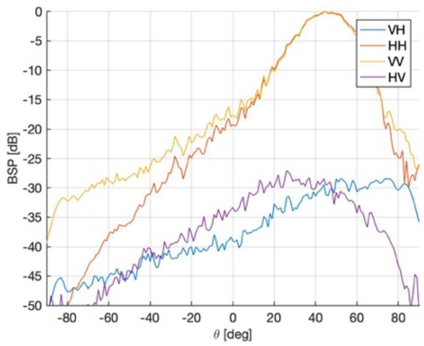

Fig. 8. Bi-static scattering from a rough surface with exponential PDF. The surface RMS height equals 0.1 mm.

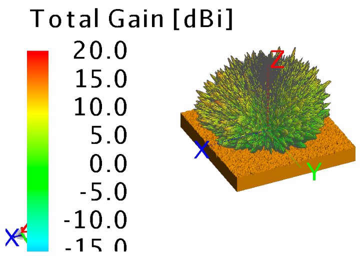

Fig. 9. Visualization of 3D bi-static scattering pattern for the surface with exponential PDF; horizontally polarized field incident at -45 degrees.

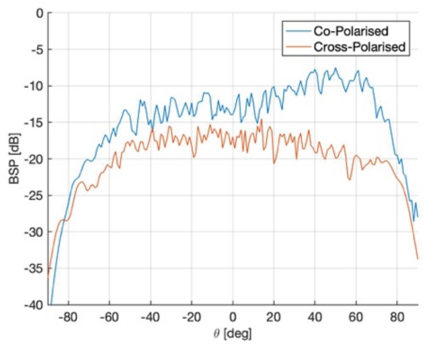

Fig. 10. Bi-static scattering of the horizontally polarized incident wave from a rough surface with exponential PDF.

IV. Conclusions

The computational approach [10] for full-wave simulations of scattering from a statistically rough surface is further developed in this paper. Application of the preconditioner before inverting the impedance matrix in the Method of Moments made the solver computationally more efficient and together with usage of more powerful computational platforms helped us to increase the size of the rough surface from 10-by-10 to at least 100-by-100 wavelengths, which essentially decreased the edge diffraction and consequently substantially increased the dynamic range of the numerical results. This surface size increase has permitted widening of the range of incident angles from almost normal as in [10] up to grazing angles. Implementation of Maxwell-compatible tapered incident wave instead of very narrow Gaussian beam allowed to compute correctly the statistical moments of the scattered field, as the incident field footprint size has been increased from 3 characteristic surface correlation lengths (which was insufficient for statistical characterization) to more than 15. A newly proposed generator of rough surfaces allows for creating a statistical ensemble of surfaces not only with a given surface correlation function, but also with an arbitrary cumulative density function, which extends applicability of the numerical model to realistic surfaces.

The results of the numerical analysis from moderately rough surfaces (RMS height equals to the half wavelength and the average value of the surface slope close to one) demonstrate the importance of multiple scattering mechanism already by 45 degrees incident angle: the co- and cross-polarized backscattered fields have very similar values, which have never been shown by all available (semi-)analytical models of scattering from rough surface. Also the bi-static scattering pattern for the same class of surfaces exhibits almost isotropic scattering in all directions (similar to Lambert law). Finally, influence of surface PDF on the bi-static scattered power is demonstrated for the first time.

The numerical model extension to statistically rough dielectric interfaces will be presented elsewhere.

References

[1] W. Bouwmeester, F. Fioranelli, and A. Yarovoy, “Dynamic Road Surface Signatures in Automotive Scenarios”, Proc. 18th European Radar Conference (EuRAD), London, United Kingdom, 2022.

[2] P. Beckmann and A. Spizzichino, The Scattering of Electromagnetic Waves from Rough Surfaces, Goford: Pergamon Press, 1963.

[3] A .Voronovich, “Small-slope approximation for electromagnetic wave scattering at a rough interface of two dielectric half-spaces,” Waves Random Media, vol. 4, pp. 337-367, 1994.

[4] A. G. Yarovoy, "Small-slope iteration technique for wave scattering from a rough interface of two media," IEEE Trans. Antennas and Propagation, vol. 44, no. 11, pp. 1433-1437, Nov. 1996.

[5] H. Rudolf, G. Wanielik, and A.J. Sieber, “Road condition recognition using microwaves,” In Proceedings of Conference on Intelligent Transportation Systems, pp. 996–999, 1997.

[6] K. Sarabandi, E.S. Li, and A. Nashashibi, “Modeling and measurements of scattering from road surfaces at millimeter-wave frequencies,” IEEE Trans. Antennas and Propagation, vol. 45, pp. 1679–1688, Nov. 1997.

[7] E. Li and K. Sarabandi, “Low grazing incidence millimeter-wave scattering models and measurements for various road surfaces,” IEEE Trans. Antennas and Propagation, vol. 47, no. 5, pp. 851–861, May 1999.

[8] V.V Viikari et al. “Road-condition recognition using 24-GHz automotive radar,” IEEE Trans. Intelligent Transportation Systems,” vol. 10, pp. 639–48, April 2009.

[9] A. Bystrov, E. Hoare, T. -Y. Tran, N. Clarke, M.Gashinova, and M. Cherniakov, “Sensors for automotive remote road surface classification,” 2018 IEEE Int. Conf. Vehicular Electronics and Safety (ICVES), pp. 1–6, 2018.

[10] R.L. Wagner, J. Song, and W.C. Chew, “Monte Carlo simulation of electromagnetic scattering from two-dimensional random rough surfaces,” IEEE Transactions on Antennas and Propagation, vol.45, pp. 235–245, Feb. 1997.

[11] E.I. Thorsos, “An Examination of the 'Full-Wave' Method for Rough Surface Scattering: Part II,” National Radio Science Meeting, Boulder, Colorado, Jan.1989.

[12] Altair Feko 2022.3. Altair Feko User Guide. URL: https://help.altair.com/feko/pdf/Altair_Feko_User_Guide.pdf.

[13] S. J. Orfanidis, Electromagnetic Waves and Antennas, 1999. Available at www.ece.rutgers.edu/orfanidi/ewa, 1999.